Journal of Applied Pharmaceutical Research
Volume 13 Issue 4, Year of Publication 2025, Page 239 –253
DOI: https://doi.org/10.69857/joapr.v13i4.1322

Check for updates

Research Article

JOURNAL OF APPLIED PHARMACEUTICAL RESEARCH | JOAPR
www.japtronline.com ***ISSN: 2348 – 0335***

DESIGN, OPTIMIZATION, AND ANTIMICROBIAL ASSESSMENT OF CALLICARPA LONGIFOLIA-DERIVED NANOPARTICLES USING QUALITY BY DESIGN (QbD) APPROACH

Md. Shakeel Alam*, Nidhi Srivastava

Article Information
Received: 9th May 2025
Revised: 17th July 2025
Accepted: 6th August 2025
Published: 31st August 2025

Keywords
Callicarpa longifolia-derived nanoparticles, Box-Behnken Design, Isolated extract fraction, Drug release, antibacterial study.

ABSTRACT
Background: The purpose of this study is to focus on the design, optimization, and antimicrobial evaluation of ethanolic leaf extracts of *Callicarpa longifolia*-derived nanoparticles using the Quality by Design (QbD) technique. **Methodology:** Critical formulation parameters were optimized using a Box-Behnken Design. The optimized nanoparticles are characterized using Dynamic Light Scattering (DLS), Zeta Potential analysis, and Scanning Electron Microscopy (SEM), confirming their nanoscale size. Stability studies were conducted under various ICH recommendations. The antimicrobial activity of the isolated fraction extract and isolated fraction extract nanoparticles was assessed against Gram-positive (*Staphylococcus aureus*) and Gram-negative (*Escherichia coli*) bacteria using the agar well diffusion method. **Results and Discussion:** By BBD, the optimized herbal nanoparticles have a particle size of 281.00 nm and an entrapment efficiency 88%. After characterization, the results of the optimized nanoparticles' particle size (349.3 nm), zeta potentials (-23.7 mV), % EE (86.25%), and spherical shape are confirmed by SEM. The % cumulative drug release of optimized nanoparticles is 86.12±0.79. Kinetic release model regression values of the optimized nanoparticles' R^2 values in different model kinetic releases are zero order (0.929), first order (0.971), Higuchi kinetic release (0.994), Korsmeyer kinetic release (0.994), and Hixon Crowell (0.978). Results revealed that the nanoparticle formulation exhibited significant antimicrobial efficacy. **Conclusion:** All things considered, the study shows how the QbD methodology may be successfully applied to create a stable and efficient nanoparticle system made from an isolated extract of *C. longifolia*, which has encouraging potential as a substitute antibacterial agent.

INTRODUCTION

Globally, herbal treatments have been an essential part of traditional medicine, and their ability to heal a wide range of illnesses continues to get international acclaim. These treatments are derived from plants and frequently contain a complex variety of bioactive components, such as polyphenols, terpenoids, alkaloids, and flavonoids, which contribute to their pharmacological effects. Chronic illnesses like diabetes, liver problems, heart disease, and infections have all been successfully treated with them [1-3]. Herbal medicines present

*Maharshi University of Information Technology (Department of Pharmacy) Sitapur Road, P.O. Maharishi Vidya Mandir, Lucknow-226013 (Uttar Pradesh), India

***For Correspondence:** **rehan0339@gmail.com**

prospective substitutes or supplements to traditional therapies, bolstering the global shift toward holistic and personalized medicine as they gain more scientific confirmation and are included in contemporary healthcare [4-6]. *Callicarpa longifolia (C. longifolia)* is distinguished by its brilliant violet berry clusters, tiny purple blooms, and lance-shaped green leaves, belonging to the family Lamiaceae. It is indigenous to tropical and subtropical regions of Asia, which include China, India, Malaysia, and Thailand. It grows best in sunny, well-drained environments like as hills and lowland woods. It is employed in landscaping and forestry initiatives because of its versatility and ornamental attractiveness [7]. Because it contains bioactive substances like flavonoids, terpenoids, and phenolic acids, *C. longifolia* has been thoroughly investigated for its wide range of therapeutic characteristics. *C. longifolia* extracts have shown strong antibacterial and antifungal activities against several pathogens, which backs up its traditional use in treating illnesses [8]. The methanolic and ethanolic *C. longifolia leaf extract* demonstrates significant DPPH and ABTS free radical scavenging activities, which can be ascribed to their elevated phenolic content. *C. maingayi* extract fractions were evaluated and reported 14 phenylpropanoids and 6 flavones [9]. The genus "Callicarpa" has a wide range of secondary metabolites, particularly terpenoids (monoterpenoids, sesquiterpenoids, diterpenoids, and triterpenoids), flavonoids, phenylethanoids, and phenylpropanoids. From a phytochemical standpoint, many significant aspects of this genus demand specific attention: (a) The leaves, stems, and roots are the most common plant components examined for bioactive chemical isolation. (b) Terpenoids, specifically diterpenoids and triterpenoids, are the most prevalent secondary metabolites observed in this species. (c) The most common flavonoid class is multimethoxylated flavonoids, which are found in several species [10]. Nanotechnology enhances the effectiveness of herbal medicines by addressing key issues, such as the dissolution, stability, and absorption of plant ingredients. Nano-formulations, which include nanoparticles, liposomes, nano-emulsions, and phytosomes, increase systemic absorption and allow for targeted administration to specific areas, boosting efficacy while lowering side effects [11-14]. Nano-formulations provide controlled and prolonged medication release, improve the stability of active substances against environmental degradation, and allow for the passage of biological barriers such as the blood-brain barrier. Furthermore, nanotechnology permits the creation of diverse dosage forms such as transdermal patches, nasal sprays, and injectables, expanding the use of herbal remedies and enhancing adherence by patients [15-17]. Nanotechnology significantly enhances the pharmacokinetic and pharmacodynamic profiles of herbal drugs, thereby transforming traditional herbal therapies into more efficient, safe, and patient-friendly treatments [18,19]. The encapsulation of herbal bioactive components in poly (lactic-co-glycolic acid) (PLGA) nanoparticles is widely employed in pharmaceutical research because it combines herbal compounds' medicinal potential with PLGA's biocompatibility and controlled-release capabilities. It is helpful in herbal nanoparticle creation for the following reasons: increased stability of herbal actives, improved bioavailability, controlled and sustained release, targeted delivery potential, reduced toxicity and side effects, and regulatory and biocompatibility advantages [20-22]. An organized, science-based approach to pharmaceutical development, Quality by Design (QbD) places a strong emphasis on predetermined goals, in-depth knowledge of the product and process, and the application of strong process controls that are informed by good scientific principles and risk management techniques. This methodology improves the dependability and reproducibility of herbal formulations, reduces batch-to-batch variability and failures, and makes it easier to comply with increasingly demanding regulatory criteria, all of which promote the development of high-quality herbal therapies [23-25]. Encapsulation in PLGA nanoparticles is thought to improve antimicrobial activity by shielding actives from degradation, enhancing cellular absorption, and allowing for regulated release, resulting in sustained inhibitory concentrations at the infection site. This method bridges the current gap in converting *C. longifolia's* bioactive potential into an effective and stable antibacterial formulation. The current study used a Quality by Design (QbD) strategy to create nanoparticles from leaf extract, which were then thoroughly tested for antibacterial efficacy. To the best of our knowledge, no previous reports of such an investigation exist. The research strategy was based on existing literature; however, the methodological technique used was original and innovative.

MATERIALS AND METHODS

PLGA (CDH), Fraction F (Isolated from the plant extract), Poly vinyl alcohol (Loba Chemie), Di-chloromethane (Merck), and distilled water. Instruments and Glassware: HPLC (Model No. AF 2489 series) of the company Waters, Thermometer (Model No.EC-508) of company VM Electronics, Weighing Balance

(Model No. PioneerPAG213) of company OHAUS, Magnetic Stirrer & Sonicator of company Remi, and Beaker (250 ml), Conical Flask (250 ml), and Pipette of company Borosilicate. Bacterial strains and culture conditions -The bacteria used in this study were *E. coli* MTCC 42, and Staphylococcus aureus MTCC 10787. Bacteria were cultured in Nutrient Agar Media (NAM).

Extraction and Isolation

Using petroleum ether, the dried leaves of *C. longifolia* were first defatted. A Soxhlet apparatus was then used to extract the defatted material using a hydroalcoholic solvent. For 8 to 10 hours, the extraction procedure was kept at a temperature between 40 and 60°C. Following completion, the extract was dried out by filtering and concentrating. Stored the dried extract in an airtight container for later use [26]. To isolate the fraction of extract obtained by column chromatography, the hydroalcoholic extract of leaves of *C. longifolia* was subjected to silica gel column chromatography. One gram of extract was loaded, and elution was performed using a gradient solvent system of toluene: ethyl acetate: acetic acid (8:4:0.4). Used gradient solvent system of toluene: ethyl acetate: acetic acid (8:4:0.4) to performed the isolation, loaded 1 gm of extract on column chromatography, collected fractions were concentrated and further used for nanoparticles preparation [27].

Preparation and formulation of nanoparticles

To ensure full dissolution of the polymer, dissolve 100 mg of PLGA and the separated fraction (20 mg depending on load) in DCM (2.0-2 mL). To make the extract more soluble in DCM, warm it briefly or pre-dissolve it in a tiny amount of ethanol before adding it to DCM (ethanol should be less than 10% v/v of the organic phase). Prepare a 10 mL PVA solution (1.0% w/v) in a beaker and cool in an ice bath if feasible. After developing an oil-in-water (o/w) emulsion by adding the resultant organic phase dropwise to an aqueous poly (vinyl alcohol) (PVA) solution, the mixture was homogenized at 1,500 rpm to develop nanodroplets. A colloidal suspension of PLGA nanoparticles (NPs) was obtained by transferring the emulsion to a magnetic stirrer and continually stirring it at room temperature until the organic solvent had evaporated entirely. To get rid of any remaining PVA or unencapsulated medication, precisely determined aliquots of the nanoparticle suspension were centrifuged at 15,000 rpm for 15 minutes at 4°C and then rinsed twice with distilled water [28,29]. Three independent production batches (Batch A, B, and C) were created on different days to test inter-batch repeatability. Three technical duplicates (n = 3) were prepared from the identical starting materials and processed in parallel to measure intra-batch repeatability, resulting in a total of nine formulations per condition.

Optimizations of prepared nanoparticles using Box Behnken Design (BBD)

Using the BBD tool, the optimization of isolated extract nanoparticles (NPs) was performed. Subsequently, the optimized formulation was used for further characterization of BBD using Design-Expert software (version XX, Stat-Ease Inc., Minneapolis, USA). File Version 12.0.1.0 has been used for Response Surface Study (RSS) with Randomized subtype and Quadratic Design Model and Build Time (ms) 245.00 [30-32]. 3 factors, at 3 levels, were considered in the BBD experiment, for two responses, a total of 13 formulations were observed. The independent factors for this optimization are PLGA (X1), PVA concentration (X2), and stirring rpm(X3) (Table 1). Two responses for this optimization are particle size (Y1) and entrapment efficiency (Y2). The three levels are low (-1), middle (0), and high (+1). (Table 2).

Optimization of the formulation

The drug fraction (5 mg) & PLGA (125 mg) were dissolved in varying volumes of dichloromethane (DCM, 10 ml) to prepare the optimal formulation. The drug & polymer were then completely dispersed by sonicating them for 3 min. in an ultrabath sonicator. After that, portions of this solution were incorporated into a Poly Vinyl Alcohol (PVA) solution to create an o/w emulsion, which was homogenized at 1500 rpm to break it down into nanodroplets. To develop the colloidal suspension of nanoparticles (NPs), the generated emulsion was transferred to a magnetic stirrer and swirled until the organic phase completely evaporated under air conditions. The mixture was cleaned 2 times with distilled water, after centrifuging the NPs suspension precisely for 15 minutes at 4°C at 15000 rpm [33,34].

CHARACTERISATION OF NANOPARTICLES [35-37]

Particle size, polydispersity index (PDI), and zeta potential

All were measured using a Malvern Zetasizer Nano ZS at 25 ± 0.5 °C (173° backscatter angle) after diluting samples in ultrapure water (size/PDI) or 1 mM KCl. Each formulation was tested in triplicate per batch, with three different batches (n = 9). The instrument's calibration was confirmed with NIST-traceable polystyrene beads and zeta standards.

Table 1: Level of independent factors

Factors	Level		
	Low (-1)	**Middle (0)**	**High (+1)**
PLGA (mg)	05	15	25
PVA (%)	0.5	1.25	02
Stirring (min)	1000	1250	1500

Determination of the drug Entrapment Efficiency (%EE): To ensure total dissolution, a specific amount of the sedimented NPs was dissolved in 1 mL of methanol and sonicated for 2 minutes in a bath ultrasonicator. A UV-Vis spectrophotometer (Shimadzu 1900, Tokyo, Japan) was then used to perform a spectrophotometric analysis of the resultant solution against a blank formulation. The following formula was used to determine the entrapment efficiency (EE, %) after all measurements were made in triplicate, λmax 288 nm.

$$\%\ \boldsymbol{Entrapment\ Efficiency} = \frac{\boldsymbol{Wc}}{\boldsymbol{Wt}} \times \mathbf{100}$$

Where, (Wc) = amount of drug content (entrapped), (Wt)=total amount of drug in the dispersion

Calibration and validation curves included 5-7 concentration points from the predicted range (e.g., 0.5-100 μg·mL^{-1}) with linearity $R^2 \geq 0.99$. The method was validated using the following ICH Q2(R1) parameters: linearity, LOD/LOQ, specificity, accuracy (95-105% recovery), precision (intra/inter-day RSD ≤5-7%), and robustness. Each sample was injected three times; formulation statistics were calculated using three technical replicates per batch and three separate batches (n = 9). Report data as mean ± SD and percentage RSD.

Table 2: Independent Variables and Dependent Variables for the optimization of nanoparticles.

	Name	Minimum	Maximum	Mean	Std. Dev.
Independent Variables (Factors)	**PLGA mg)**	5.00	25.00	15.00	8.16
	PVA (%)	0.5000	2.00	1.25	0.6124
	Stirring (rpm)	1000.00	1500.00	1250.00	204.12
Dependent Variables (Response)	**Particle size (nm)**	229	398	334.92	54.86
	Entrapment efficiency (%)	64	88	75.62	8.08

SEM analysis

Examining the surface morphology and particle size of the nanoparticles requires the use of SEM. Lyophilized nanoparticles were mounted on aluminum stubs with double-sided carbon tape, sputter-coated with a 20nm Au/Pd layer, and scanned with a field-emission SEM (FE-SEM) with secondary-electron detection at 15 kV accelerating voltage and 10 mm working distance. Images for each formulation were collected from ≥10 random fields across three different batches; typical micrographs are displayed. Scale bars and instrument settings are shown in the figure legend.

In Vitro Release and Release Kinetics Studies

Using UV-Vis spectroscopy at 288 nm to quantify the drug, the release profile of the NPs was examined. Two distinct media were made to preserve sink conditions: 0.1 N HCl and a pH 5.5 buffer made up of 40% methanol and 60% acetate buffer. In short, an established number of lyophilized NPs suspended in 5 mL of the release medium was placed into a dialysis bag, and the final volume was set at 20 mL. After that, the apparatus was incubated for 72 hours at 37 °C and 100 rpm on an orbital shaker. At certain intervals, samples were taken out and promptly replaced with an equivalent volume of brand-new medium. For every sampling point, the total amount of extract released (mg/mL) was determined & then converted to cumulative % release. Data were processed using zero-order, first-order, Higuchi, Korsmeyer–Peppas, Hixson–Crowell, Weibull & Noyes–Whitney Equations to examine the kinetic profile from PLGA NPs [38-40].

Stability study

Following ICH guidelines, stability testing has been performed. Three months have kept the optimized NPs at two different conditions**,** 25°C ± 2°C & 60%±5% RH and 40°C±2°C & 70±5% RH. [41].

Antimicrobial activity by the Well diffusion assay

Using Nutrient Agar Medium (NAM) plates, the agar well diffusion method was employed to evaluate the antibacterial activity of isolated plant extract NPs and isolated plant extracts. The NAM was made by dissolving 28 grams of nutritional agar powder in one liter of distilled water, and before sterilizing, the pH was measured. After that, the medium was autoclaved for 15 minutes at 121°C and 15 psi. Following autoclaving, the medium was transferred onto sterile Petri dishes and left to harden under a laminar air flow. To achieve a turbidity that was equal to 0.5 McFarland standard (~1.5×10^8 CFU/mL), test microorganisms were inoculated into nutritional broth and cultured for a whole

night at 37°C. Wells (5–6 mm in diameter) were made in the solidified agar plates using a sterile cork borer. A sterilized glass spreader was used to equally distribute a 100 µL aliquot of the standardized bacterial inoculum across the agar surface. Next, the test sample (isolated extract and NPs formulations) was added to two wells that had been bored into each inoculation plate. The plates were incubated at 37°C for 24 hours after a 30-minute diffusion period at room temperature. The diameter of the clear zones of inhibition (in mm) encircling each well was used to measure the antibacterial activity [42-46].

RESULTS AND DISCUSSION

Optimizations of Nanoparticles via Box Behnken Design

The nanoparticle of leaf extract has been optimised using the BBD technique, which took into account three factors and two responses. Table 3, shows the effects of various independent variables on response parameters, particle size, and entrapment efficiency. The software has built 13 different formulations. The impacts of independent variables on dependent variables are discussed using various response surface data, including contour plots, 3D & predicted vs. actual value. The ANOVA model analysis gave favourable results. Response surface analysis was used to visually illustrate the interactions among the independent variables and their aggregate influence on the dependent variables, using 3D response surface plots and 2D contour plots. These figures have helped us gain a thorough grasp of the optimization environment and identify crucial factor-response linkages.

Table 3: Optimizations of the nanoparticle by the Box Behnken Design method.

S. No.	Factors			Response	
	A: PLGA (mg)	B: PVA (%)	C: Stirring Time (min.)	Particle size(nm)	Entrapment efficiency(%)
1	5	1.25	1500	229	82
2	25	1.25	1500	289	86
3	5	2	1250	315	78
4	25	0.5	1250	348	75
5	15	2	1500	281	88
6	5	0.5	1250	336	72
7	5	1.25	1000	389	66
8	25	1.25	1000	396	64
9	15	0.5	1000	388	67
10	15	0.5	1500	271	86
11	15	1.25	1250	337	77
12	15	2	1000	398	69
13	25	2	1250	377	73

(a) Particle size: F-value of 47.19 indicates that the model is highly significant, with only a 0.01% probability that this large F-value could occur due to noise. The p-values less than 0.0500 are considered significant; in this case, factors A and C are significant model terms. p-values greater than 0.1000 are regarded as nonsignificant. If the model contains many insignificant terms (except those required for supporting model hierarchy), model reduction may enhance its predictive capability. Furthermore, because their difference is smaller than 0.2, the Predicted R^2 of 0.8682 and the Adjusted R^2 of 0.9203 are in good agreement. The signal-to-noise ratio is 18.683, indicating an appropriate signal. All of these findings support the model's significance and dependability for navigating the design space. (Table 3).

Table 3: ANOVA Model and Fit statistic for particle size and Entrapment efficiency

Model	Responses	Std. Dev.	R^2	Adjusted R^2	Predicted R^2	F-Value	p-value	Remark
Linear	Particle Size	15.49	0.9402	0.9203	0.8682	47.19	<0.0001	Suggested
Quadratic	Entrapment efficiency	0.8165	0.9974	0.9898	0.8982	130.18	0.0010	Suggested

Final Equation (Coded Factors)

$$\boldsymbol{Particle\ size} = +334.92 + 17.62\,A + 3.50B - 62.63\,C$$

The reaction at specific amounts of each factor can be predicted using the equation expressed in terms of coded factors. Conventionally, factors are coded as +1 (high level), 0 (middle), and -1 (low level). Because the amount of the coefficients directly represents the strength of each factor's effect on the response, this coded equation is beneficial for assessing the relative influence of each factor.

Final Equation (Actual Factors)

$$\boldsymbol{Particle\ size} + \mathbf{615.77724} + \mathbf{1.76250}\ \boldsymbol{PLGA} + \mathbf{4.66667}\ \textit{PVA-0.250500 STIRRING TIME}$$

The reaction at particular levels of each factor can be used to predict the equation in terms of actual factors; for this, each factor must be expressed in original units. The response surface, data in the form of images for the particle size of optimised formulation in terms of a graph of predicted vs actual value (a), contour plot (b), 3D response (c) & overlay plot (d) are presented in Figure 1.

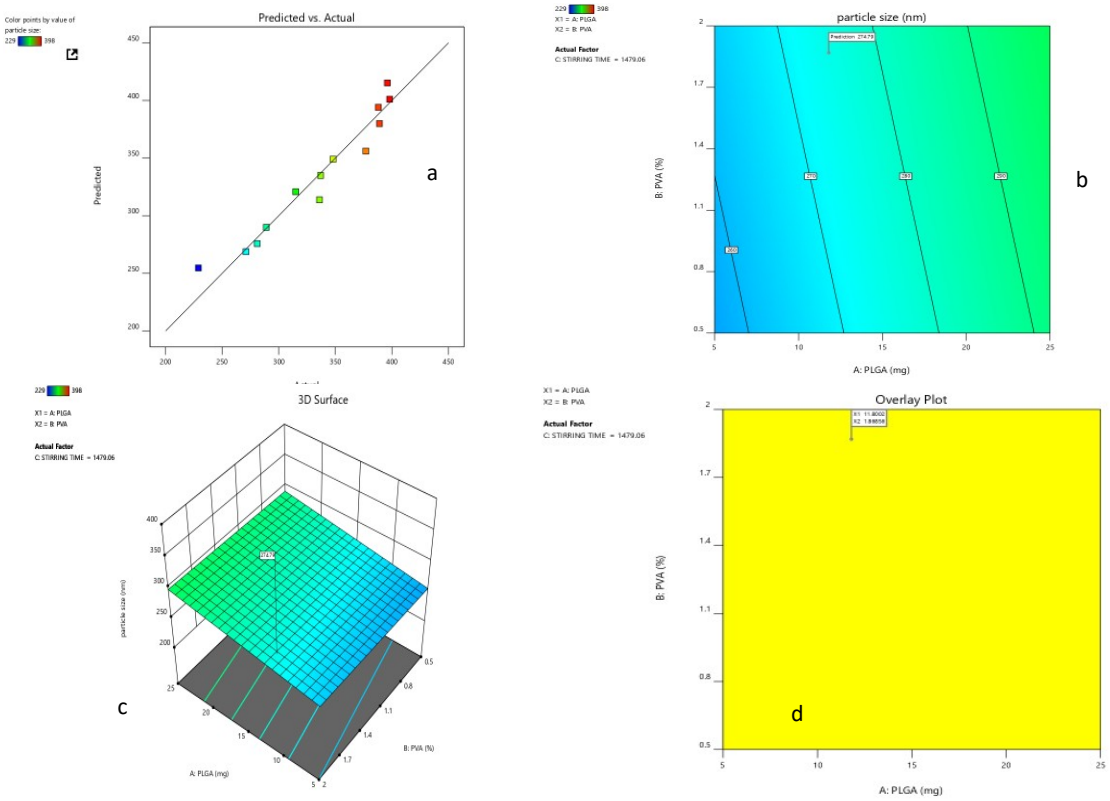

Figure 1: Response surface plot for particle size (a) Predicted vs actual value (b) Contour Plot (c) 3 D (d) overlay plot.

(b) Entrapment efficiency: Highly significant model, as indicated by its F-value (130.18). The F-value of this size, which may be caused by random noise, is a mere 0.10%. The terms B, C, AB, AC, and A^2 are significant in this model; terms with a p-value less than 0.0500 are regarded as statistically significant. Additionally, 34.212 is the value of the signal-to-noise ratio, which is greater than 4, validating a strong signal. (Table 3).

Final Equation in Terms of Coded Factors:

$$\boldsymbol{Entrapment\ efficiency} = +\mathbf{77.00} + \mathbf{0.0000}\ \boldsymbol{A} + \mathbf{1.0000}\ \boldsymbol{B} + \mathbf{9.50}\ \boldsymbol{C} - \mathbf{2.00}\boldsymbol{AB} + \mathbf{1.50}\ \boldsymbol{AC} + \mathbf{0.0000}\ \boldsymbol{BC} - \mathbf{2.75}\ \boldsymbol{A^2} + \mathbf{0.2500}\boldsymbol{B^2} + \mathbf{0.2500}\ \boldsymbol{C^2}$$

The reaction at specific amounts of each factor can be predicted using the equation expressed in terms of coded factors. Conventionally, the factors' high and low levels are denoted by the codes +1 and -1, respectively. Because the coefficients in this coded equation accurately represent the magnitude of each factor's impact on the response, it is beneficial for assessing the relative influence of the components.

Final Equation in Terms of Actual Factors:

$$\boldsymbol{Entrapment\ efficiency} = +\mathbf{34.84028} + \mathbf{0.408333}\ \boldsymbol{PLGA} + \mathbf{4.22222}\ \boldsymbol{PVA} + \mathbf{0.019000}\ \boldsymbol{Stiring\ time} - \mathbf{0.266667}\ \boldsymbol{PLGA} * \boldsymbol{PVA} + \mathbf{0.000600}\ \boldsymbol{PLGA} * \boldsymbol{Stirring\ time} + \mathbf{2.34264E-18}\ \boldsymbol{PVA} * \boldsymbol{Stirring\ time} - \mathbf{0.027500}\ \boldsymbol{PLGA^2} + \mathbf{0.444444}\ \boldsymbol{PVA^2} + \mathbf{4.00000E-06}\ \boldsymbol{Stirring\ time^2}$$

For specific levels of each factor, predictions regarding the reaction can be made using the equation expressed in terms of actual factors. In this case, each factor's levels should be stated in its original units.The response surface, data in the form of images for the Entrapment efficiency of optimised formulation in terms of graph of predicted vs actual value (a), contour plot (b), 3D response (c), and overlay plot (d) are presented in Figure 2. The desirability response surface of both dependent variables is presented in Figure 3, the predicted value of the independent variables in Table 4, and the dependent variables in Table 5.

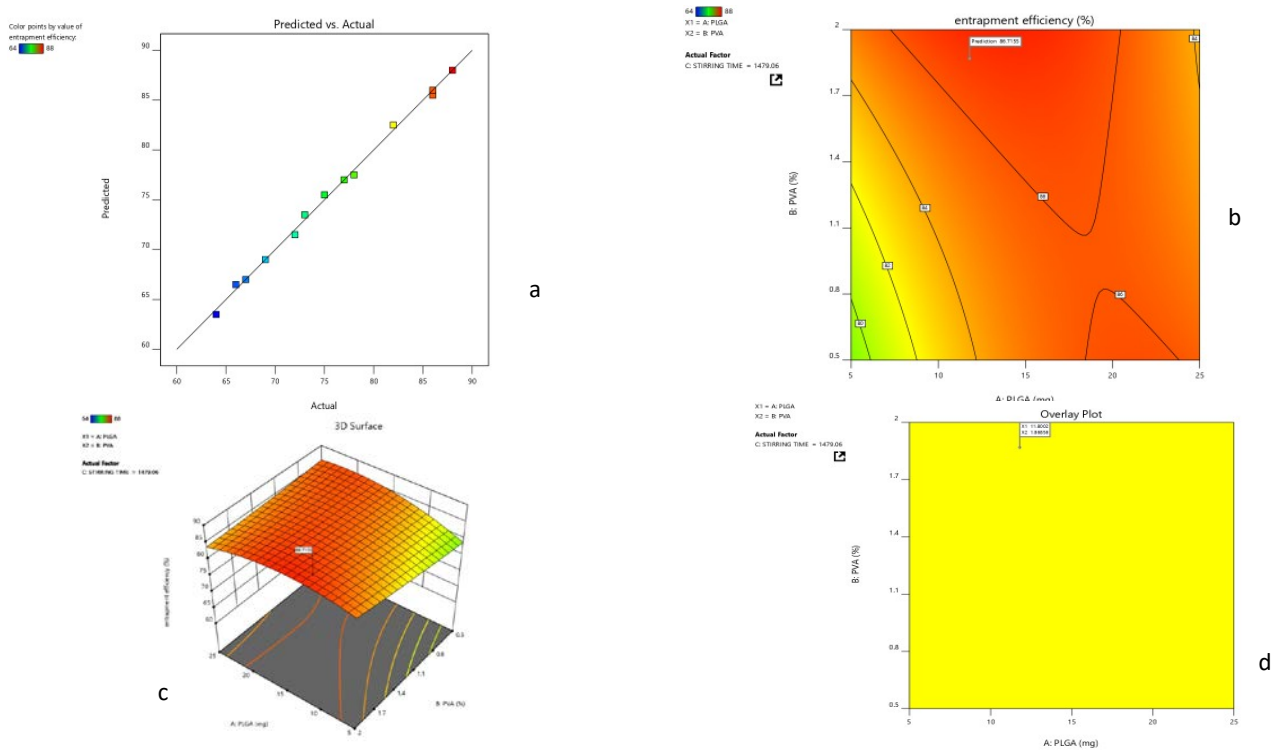

Figure 2: Response surface plot for EC (a) Predicted vs actual value (b) Contour Plot (c) 3 D (d) overlay plot.

Table 4: Predicted value of independent variables.

Factors	Level	Low level	High level	Std. Dev.	Coding
PLGA	11.80	5.00	25.00	0.0000	Actual
PVA	1.87	0.5000	2.00	0.0000	Actual
Stirring Rate (RPM)	1479.06	1000.00	1500.00	0.0000	Actual

Table 5: Predicted value of dependent variables.

Response	Predicted Mean	Predicted Median	Std. Dev.	SE mean	CI low (95%)	CI high (95%)	95 % TI low for 99% Pop	95 % TI high for 99% Pop
Particle size (nm)	274.79	274.79	15.4872	8.19043	256.262	293.318	194.146	355.435
Entrapment efficiency(%)	86.7155	86.7155	0.816497	0.60561	84.7881	88.6428	79.149	94.2819

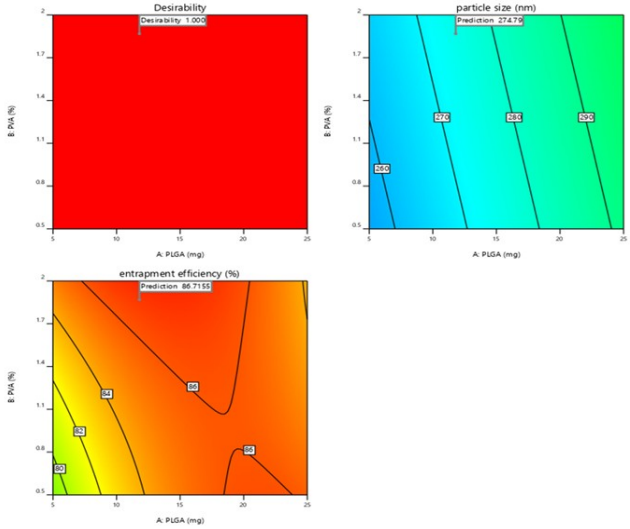

Figure 3: The desirability response surface of both dependent variables.

Increased PLGA concentration resulted in bigger particle size, most likely because of the organic phase's higher viscosity, which limits droplet breakdown during emulsification and promotes coalescence [47]. Higher PLGA concentrations also improved encapsulation efficiency (EE), since a denser polymer matrix better entraps the medication and lowers diffusion losses during preparation [48]. Increasing PVA concentration lowered particle size by improving emulsion droplet stabilization; nevertheless, excessive PVA may increase particle size by forming a thicker interfacial layer [49]. Higher stirring speed decreased particle size by increasing shear forces that produce finer emulsions; however, excessively high speeds can lower EE by promoting drug diffusion into the aqueous phase [50].

Optimized formulation

The drug fraction (5 mg) and PLGA (15 mg) were mixed in 10 mL of dichloromethane (DCM) to develop the optimum formulation. The isolated extract (drug), and polymer were then completely dissolved by sonicating them for 3 minutes in a bath ultrasonicator. In order to create an oil-in-water (o/w) emulsion, the resultant organic solution was then added dropwise to a polyvinyl alcohol (PVA) solution while being continuously stirred. The resulting o/w emulsion was then homogenized at 1,500 rpm to reduce the droplets to the nanoscale range. In order to create the colloidal suspension of PLGA nanoparticles (NPs), the generated emulsion was subsequently moved to a magnetic stirrer and swirled until the organic phase completely evaporated under air conditions. Following two washes with distilled water, precisely measured portions of the NP suspension were centrifuged at 15000 rpm for 15 min at 4°C.

CHARACTERISATION OF THE NANOPARTICLES

Particle Size and Zeta potential determination: Dynamic Light Scattering (DLS) research showed that the produced nanoparticles had a hydrodynamic diameter of 349 nm, indicating a relatively uniform size distribution (Figure 4a). The hydrodynamic diameter is an essential parameter in nanoparticle characterisation because it determines their pharmacokinetics, cellular uptake, and general behaviour in biological systems. Several studies have demonstrated its importance when assessing the in-living effectiveness and beneficial effects of nanoparticle-based formulations. The zeta potential analysis (Figure 4b) showed a clear peak at -23.7 mV. A zeta potential above ±30 mV indicates highly stable nanoparticle dispersions; however, the measured somewhat negative value reflects reasonable colloidal stability. The negative surface charge is most likely due to the capping action of bioorganic elements found in plant extracts, which provide electrostatic repulsion between particles, reducing agglomeration [51-53]. Notably, the experimentally measured values for particle size and zeta potential closely matched the projected outcomes established by the Design of Experiments (DoE) model, demonstrating the formulation strategy's robustness (Table 2). The particle size of our optimized herbal extract-loaded PLGA nanoparticles (281.00 nm) is within the range reported for similar systems. Existing literature has created Curcuma longa extract-loaded PLGA nanoparticles with a mean size of 210-320 nm [54] and Withania somnifera extract-loaded PLGA nanoparticles with a mean size of 250-340 nm [55]. Our encapsulation effectiveness (82.4%) is consistent with recent studies [56], which reported 78-85% for Nigella sativa extract-loaded PLGA nanoparticles. The zeta potential in our study (-23.7 mV) is comparable to values reported [57] (-21 to -26 mV) for herbal extract nanoparticles, demonstrating considerable electrostatic stability with steric contributions from PVA. These commonalities indicate that our formulation parameters and results are compatible with documented trends in herbal extract-loaded polymeric nanoparticle systems. Minor variances may be attributable to differences in extract composition, polymer ratio, and emulsification conditions.

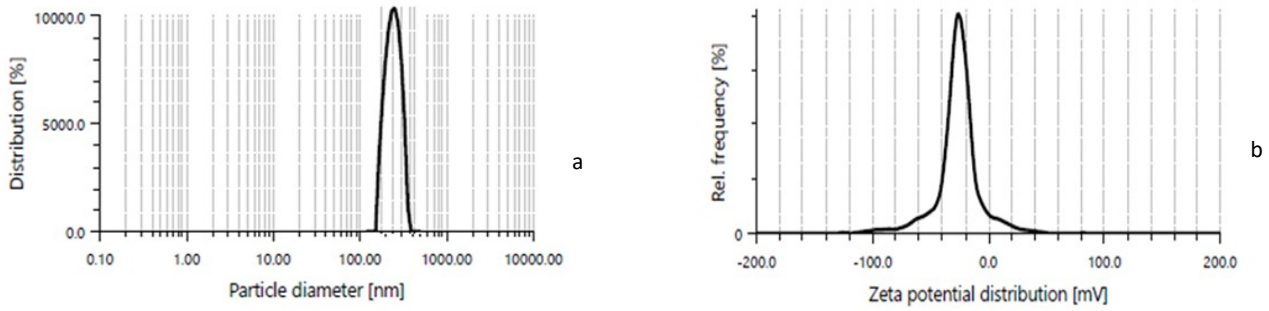

Figure 4: Optimised herbal nanoparticles (a) Particle size (b) Zeta potentials

SEM analysis: SEM examination was used to investigate the surface appearance and structural properties of the herbal isolated extract nanoparticles. The micrographs showed that the nanoparticles were spherical primarily, with a reasonably smooth surface topology. The particles seemed well-dispersed with low aggregation, indicating effective stabilization, most likely due to the presence of bioactive phytoconstituents that act as natural capping agents. The observed morphology supports the creation of nanoscale particles, which corresponds to the size distribution data acquired from DLS analysis [58] (Figure 5). These findings corroborate the efficacy of the synthesis approach and shed light on the physical properties required for biological interactions and medicinal activity.

Determination of the drug %EE: It is an essential measure for assessing the efficacy of nanoparticle-based drug delivery systems, especially for herbal extracts containing bioactive phytoconstituents. It denotes the percentage of total medication successfully encapsulated within the nanoparticle matrix as compared to the initial amount employed during formulation [59,60]. Herbal isolated fraction-loaded nanoparticles have good 86.25 % EE (Figure 6), which suggests efficient inclusion of active chemicals. The result is critical for increasing stability, bioavailability, and sustained release. The EE can be modified by several formulation variables, including the type of polymer or carrier utilized, the nature of the extract, particle size, and preparation process. A high entrapment efficiency not only reduces drug loss during processing but also improves the effectiveness of treatment by ensuring a regulated and targeted delivery profile. In this investigation, the herbal extract nanoparticles displayed significant entrapment efficiency, indicating successful phytoconstituent encapsulation and confirming the formulation's potential for improved pharmacological effects [61,62].

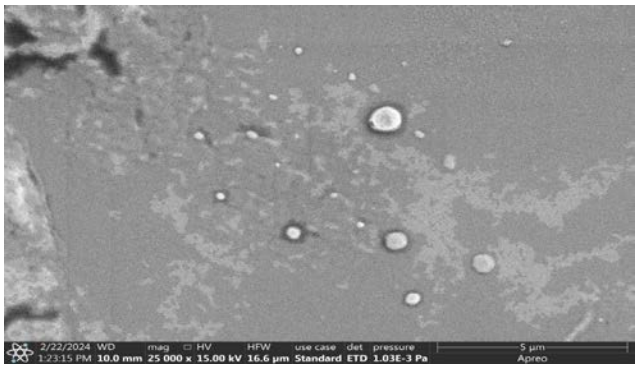

Figure 5: Surface appearance and Structural properties of optimised nanoparticle by SEM

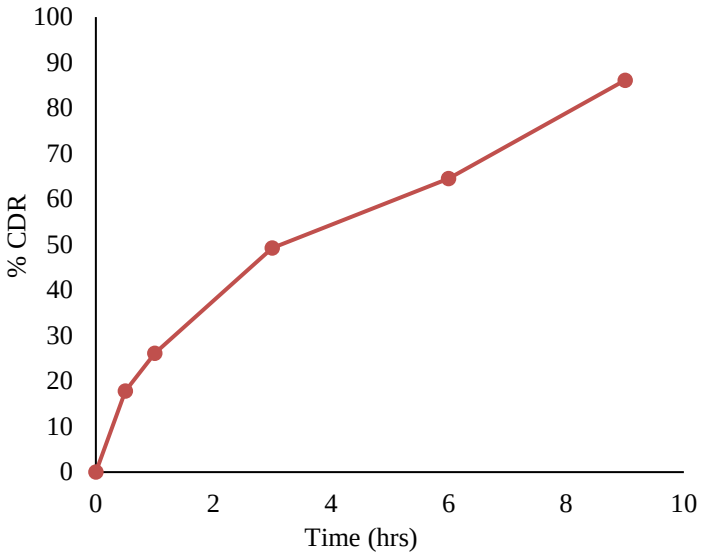

Figure 6: % cumulative drug release of the Herbal isolated fraction-loaded nanoparticles.

Drug release and kinetics studies

The cumulative drug release shows the drug released from the formulation. The cumulative percentage of drug release (%CDR) from was found to be 86.12%. The medication release from the optimized herbal nanoparticles (NPs) occurs after 9 hrs. Regression coefficients (R^2) were computed by using several kinetic models applied to the in vitro release study results (Figure 7). The medication released from the formulation under investigation had the Higuchi release model, followed by the Korsmeyer-Peppas, which had the best correlation coefficient value. Korsmeyer defines drug release from an insoluble matrix–Peppas release exponent data as the square root of a time-dependent process based on Fickian diffusion. [63,64].

Stability study

The stability of the optimised herbal nanoparticles has been examined under various storage conditions to determine their physicochemical integrity throughout time. Nanoparticles were held at several temperatures ($4 \pm 2°C$, $25 \pm 2°C$, 60% RH, and $40 \pm 2°C$, 75% RH) for up to 90 days, as per ICH standards. Changes in particle size, zeta potential, and entrapment efficiency were monitored at 0, 30, 60, and 90-day intervals. Visual observations of aggregation, colour change, and sedimentation were also documented. The findings revealed limited fluctuation in critical parameters, with no notable symptoms of aggregation or instability, especially under refrigerated and ambient circumstances. At raised temperatures and humidity, particle size decreased slightly, and zeta potential

increased, demonstrating that accelerated circumstances have a minimal effect on nanoparticle stability. As a whole, the formulation displayed good physical and colloidal stability, indicating its suitability for long-term storage and future therapeutic use [65] (Table 6).

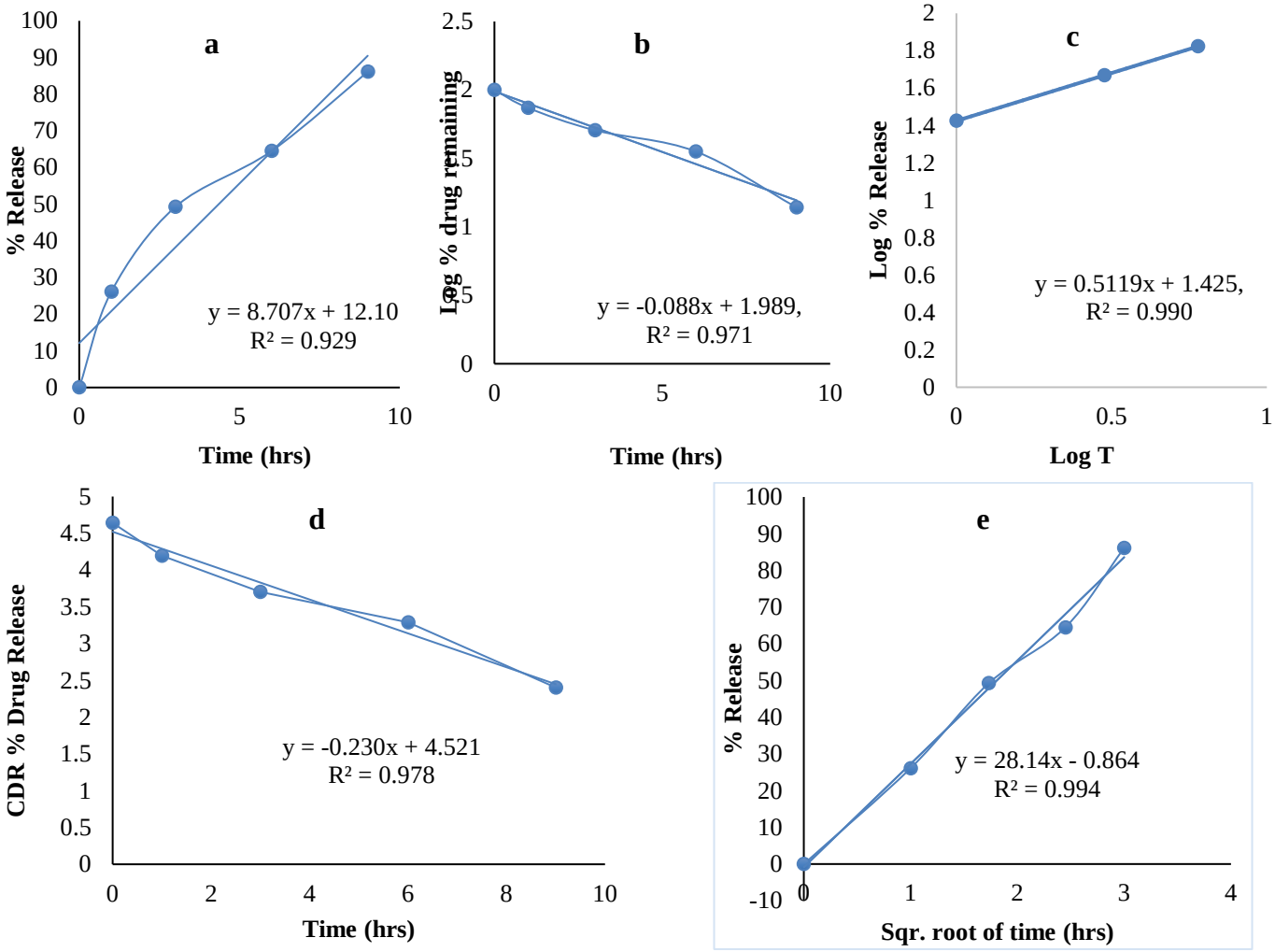

Figure 7: Different Release Kinetics of optimised formulation (a) Zero order (b) First order (c) Korsmeyer–Peppas (d) Hixon Crowell (e) Hugachi model.

Table 6: Stability of nanoparticles at different temperatures and humidity.

S. No.	(Days)	25^0±2 ^{0}C & 60 ± 5% RH			40^0C ±2 ^{0}C and 70 ±5% RH		
		Particle size	% EE	Zeta potential (mV)	Particle size	% EE	Zeta Potential
1.	**0**	349.3	86	-23.7	349.3	86	-23.7
2.	**30**	350.2	85.9	-23.9	348.9	85.9	-23.6
3.	**60**	351.2	85.88	-24.1	348.6	85.89	-23.32
4.	**90**	351.7	85.81	-24.6	347.9	85.84	-23.1

Antibacterial activity

The antibacterial activity of the produced herbal nanoparticles and standard medication was assessed against chosen bacterial strains using the agar well diffusion method. The zones of inhibition were evaluated and compared to the conventional medicines as well as the plant extract nanoparticle. The herbal nanoparticles have antibacterial activity, implying enhanced absorption and contact with microbial membranes due to their nanoscale size. Notably, the drug-loaded nanoparticles demonstrated much higher zones of inhibition against Gram+ bacteria (*S. aureus*), for nanoparticles the zone of inhibition in nm (n=3)(Mean ±SD:17.666±1.527) & for herbal isolated

extract was (Mean ± SD:12.333±1.527) and less against Gram-negative bacteria (*E. coli*), for nanoparticles the zone of inhibition in nm (n=3)(Mean ± SD: 11.33±0.577) & for herbal isolated extract was (Mean ±SD: 12±2.645) compare to standard drug (Figure 8). This therapeutic action is due to the combination of phytoconstituents & the nanoparticles, which enhances the surface area & prolonged release behavior. The improved efficacy of the nanoformulation suggests that nanoencapsulation protects the bioactivity of the herbal extract while simultaneously increasing its antibacterial potency. These findings indicate that the proposed herbal nanoparticle system has the potential to be an effective antibacterial treatment method [66].

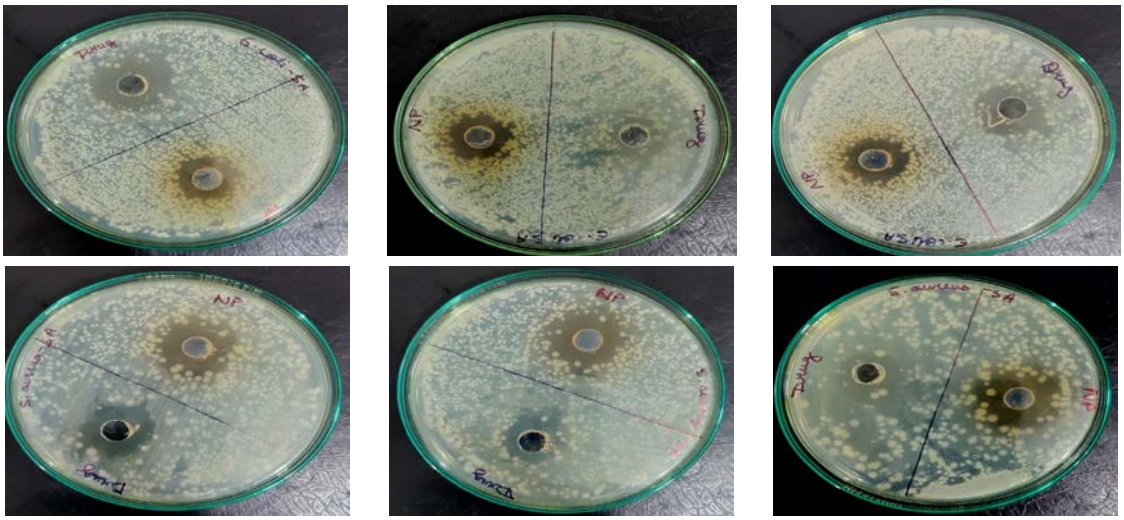

Figure 8: Antimicrobial activity of isolated fraction extract and nanoparticles against *S. aureus and E. coli.*

The antibacterial activity demonstrated in *C. longifolia* fraction-loaded nanoparticles can be attributed to bioactive phytoconstituents found in the plant. *C. longifolia* has been shown to contain alkaloids (e.g., berberine-like substances), flavonoids, tannins, and phenolic acids, all of which have antibacterial properties. Alkaloids can damage microbial cell wall integrity and limit nucleic acid production, whereas flavonoids and tannins can cause membrane permeabilization, enzyme inactivation, and metal ion chelation, resulting in microbial cell death [67,68].

CONCLUSION

The present research focuses on the development and antimicrobial assessment of nanoparticles obtained from *C. longifolia* leaf extract utilizing a BBD approach. This systematic approach ensured a thorough understanding of formulation factors (PLGA, PVA, and Stirring Time) and their impact on essential quality parameters like particle size and entrapment efficiency. The formulation parameters were adjusted using a Box Behnken Design to produce nanoparticles with desired physicochemical properties, including stability and homogeneity. Good colloidal stability was indicated by the optimized nanoparticles' narrow polydispersity index, negative zeta potential, and mean particle size in the nanoscale range. The existence of the bioactive substances that give it its antibacterial properties was confirmed by phytochemical profiling from existing literature. Common bacterial strains were used to evaluate the antibacterial activity of the nanoparticles compared to the usual medication. When compared to the usual medicine, the results indicated that the nanoparticle formulations had much higher zones of inhibition, especially against *S. aureus*, but the results for *E. coli* were lower. The greater permeability and sustained release characteristics of the nano formulation are responsible for this increased activity. To sum up, the study effectively showed that *C. longifolia*-based nanoparticles, enhanced using the QbD framework, present a viable approach to creating strong antibacterial agents. Innovative plant-based nano-formulations for the treatment of microbial infections are made possible by the combination of nanotechnology with conventional herbal medicine, which improves therapeutic efficacy. Unlike earlier studies, which either evaluated crude extracts or used standard formulation methods, our strategy combines fraction enrichment, statistical optimization, and nanoscale delivery to address solubility, stability, and bioavailability constraints. This integrated strategy not only improves *C. longifolia's* antibacterial properties but also creates

a reliable and scalable methodology for converting underutilized herbal actives into sophisticated nanotherapeutics. Yet, certain limits must be noted. The antibacterial evaluation was limited to in vitro studies, which may not accurately predict efficacy in vivo. This study did not investigate long-term stability beyond the trial period, potential cytotoxicity on mammalian cells, or detailed pharmacokinetic behaviour.

Furthermore, the scope of antimicrobial testing was confined to specific strains, and the mechanism of antimicrobial action requires further molecular investigation. Future studies should concentrate on thorough in vivo assessments, such as toxicity profiling, pharmacokinetic and pharmacodynamic tests, and broader antimicrobial screening. Examination into the molecular mechanisms of action and potential synergistic effects with traditional antibiotics could boost the therapeutic potential of *C. longifolia*-derived nanoparticles. In the end, such trials will be required to take this formulation to clinical application.

FINANCIAL ASSISTANCE
NIL

CONFLICT OF INTEREST
The authors declare no conflict of interest.

AUTHOR CONTRIBUTION
All authors participated in the work substantively and have approved the manuscript as submitted. Data collection, drafting the article, and article writing were carried out by Md. Shakeel Alam. Conceptualization or design of the work, and critical revision of the article were done by Nidhi Srivastava. All the authors have read and approved the manuscript. Each author has agreed to the publication of the manuscript.

REFERENCES
[1] Ansari P, Reberio AD, Ansari NJ, Kumar S, Khan JT, Chowdhury S, Abd El-Mordy FM, Hannan JMA, Flatt PR, Abdel-Wahab YHA, Seidel V. Therapeutic Potential of Medicinal Plants and Their Phytoconstituents in Diabetes, Cancer, Infections, Cardiovascular Diseases, Inflammation and Gastrointestinal Disorders. *Biomedicines*, **13(2),** 454 (2025) https://doi.org/10.3390/biomedicines13020454

[2] Bhoi A, Dwivedi SD, Singh D, Singh MR, Keshavkant S. Worldwide health scenario from the perspective of herbal medicine research. In Phytopharmaceuticals and herbal drugs. *Academic Press*,13-32 (2023) https://doi.org/10.1016/B978-0-323-99125-4.00014-7

[3] Oyedepo TA, Palai S. Herbal remedies, toxicity, and regulations. Preparation of Phytopharmaceuticals for the Management of Disorders. *Academic Press*, 89-127 (2021) https://doi.org/10.1016/B978-0-12-820284-5.00014-9

[4] Hassen G, Belete G, Carrera KG, Iriowen RO, Araya H, Alemu T, Solomon N, Bam DS, Nicola SM, Araya ME, Debele T, Zouetr M, Jain N. Clinical Implications of Herbal Supplements in Conventional Medical Practice: A US Perspective. *Cureus*, **14(7)**, e26893 (2022) http://dx.doi.org/10.7759/cureus.26893

[5] Javed MN, Dahiya ES, Ibrahim AM, Alam MS, Khan FA, Pottoo FH. Recent advancement in clinical application of nanotechnological approached targeted delivery of herbal drugs. *Nanophytomedicine, Concept to Clinic*, 151-72 (2020) https://doi.org/10.1007/978-981-15-4909-0_9

[6] Taleuzzaman M, Jain P, Verma R, Iqbal Z, Mirza MA. Eugenol as a Potential Drug Candidate: A Review. *Current Topics in Medicinal Chemistry*, **21(20)**, 1804-1815 (2021) https://doi.org/10.2174/1568026621666210701141433

[7] Wang CY, Chen LH, He HL, Liu Y, Wang Q. The complete chloroplast genome of *Callicarpa longifolia* Lamk. var. *floccosa* Schauer (Lamiaceae). *Mitochondrial DNA Part B*, **6(12)**, 3473-3474 (2021) https://doi.org/10.1080/23802359.2021.2002210

[8] Tourabi M, Metouekel A, Ghouizi AE, Jeddi M, Nouioura G, Laaroussi H, Hosen ME, Benbrahim KF, Bourhia M, Salamatullah AM, Nafidi HA. Efficacy of various extracting solvents on phytochemical composition, and biological properties of Mentha longifolia L. leaf extracts. *Scientific Reports*, **13(1)**, 18028 (2023) https://doi.org/10.1038/s41598-023-45030-5

[9] Yu M, Gouvinhas I, Rocha J, Barros AI. Phytochemical and antioxidant analysis of medicinal and food plants towards bioactive food and pharmaceutical resources. *Scientific reports*, **11(1)**, 10041 (2021) https://doi.org/10.1038/s41598-021-89437-4

[10] Nghakliana F, Zosangzuali M, Lalremruati M, Lalmuansangi C. Ethnopharmacological Applications and Phytochemical Compounds of the Genus Callicarpa L. Bioactives and Pharmacology of Lamiaceae *Apple Academic Press*, **1**, 343-366 (2023) https://doi.org/10.1201/9781003346142

[11] Dewi MK, Chaerunisaa AY, Muhaimin M, Joni IM. Improved Activity of Herbal Medicines through Nanotechnology. *Nanomaterials (Basel)*, **12(22)**, 4073 (2022) https://doi.org/10.3390/nano12224073

[12] Awlqadr FH, Majeed KR, Altemimi AB, Hassan AM, Qadir SA, Saeed MN, Faraj AM, Salih TH, Abd Al-Manhel AJ, Najm MA, Tsakali E. Nanotechnology-Based Herbal Medicine: Preparation, Synthesis, and Applications in Food and Medicine. *Journal of Agriculture and Food Research*, **19**, 101661 (2025) https://doi.org/10.1016/j.jafr.2025.101661

[13] Kaur J, Anwer MK, Sartaj A, Panda BP, Ali A, Zafar A, Kumar V, Gilani SJ, Kala C, Taleuzzaman M. ZnO nanoparticles of

Rubia cordifolia extract formulation developed and optimized with QbD application, considering ex vivo skin permeation, antimicrobial and antioxidant properties. *Molecules*, **27(4)**, 1450 (2021) https://doi.org/10.3390/molecules27041450

[14] Taleuzzaman M, Sartaj A, Kumar Gupta D, Gilani SJ, Mirza MA. Phytosomal gel of Manjistha extract (MJE) formulated and optimized with central composite design of Quality by Design (QbD). *Journal of Dispersion Science and Technology*, **44(2)**, 236-44 (2021) https://doi.org/10.1080/01932691.2021.1942036

[15] Dewi MK, Chaerunisaa AY, Muhaimin M, Joni IM. Improved Activity of Herbal Medicines through Nanotechnology. *Nanomaterials (Basel)*, **12(22)**, 4073 (2022) https://doi.org/10.3390/nano12224073

[16] Lopalco A, Iacobazzi RM, Lopedota AA, Denora N. Recent Advances in Nanodrug Delivery Systems Production, Efficacy, Safety, and Toxicity. *Methods Molecular Biology*, **2834**, 303-332 (2024) http://dx.doi.org/10.1007/978-1-0716-4003-6_15

[17] Sharma D, Gupta A, Rawat R, Sharma S, Yadav JS, Saxena A. Exploring nano formulation drug delivery of herbal actives for enhanced therapeutic efficacy: A comprehensive Review. *Intelligent Pharmacy*, **3(1)**, 26-34 (2024) https://doi.org/10.1016/j.ipha.2024.07.004

[18] Huang L, Luo S, Tong S, Lv Z, Wu J. The development of nanocarriers for natural products. *Wiley Interdisciplinary Reviews: Nanomedicine and Nanobiotechnology*, **16(3)**, e1967 (2024) https://doi.org/10.1002/wnan.1967

[19] Rombolà L, Scuteri D, Marilisa S, Watanabe C, Morrone LA, Bagetta G, Corasaniti MT. Pharmacokinetic Interactions between Herbal Medicines and Drugs: Their Mechanisms and Clinical Relevance. *Life (Basel)*, **10(7)**, 106 (2020) https://doi.org/10.3390/life10070106

[20] Abdul Rahim R, Jayusman PA, Muhammad N, Ahmad F, Mokhtar N, Naina Mohamed I, Mohamed N, Shuid AN. Recent Advances in Nanoencapsulation Systems Using PLGA of Bioactive Phenolics for Protection against Chronic Diseases. Int J Environ Res Public Health. **16(24),** 4962 (2019) https://doi.org/10.3390/ijerph16244962

[21] Roshan Z, Haddadi-Asl V, Ahmadi H, Moussaei M. Curcumin-encapsulated poly (lactic-co-glycolic acid) nanoparticles: a comparison of drug release kinetics from particles prepared via electrospray and nanoprecipitation. Macromolecular Materials and Engineering. 309 (7):2400040, (2024) https://doi.org/10.1002/mame.202400040

[22] Awlqadr FH, Majeed KR, Altemimi AB, Hassan AM, Qadir SA, Saeed MN, Faraj AM, Salih TH, Abd Al-Manhel AJ, Najm MA, Tsakali E. Nanotechnology-based herbal medicine: Preparation, synthesis, and applications in food and medicine. Journal of Agriculture and Food Research. **31:101661,** (2025), https://doi.org/10.1016/j.jafr.2025.101661

[23] Zagalo DM, Sousa J, Simões S. Quality by design (QbD) approach in marketing authorization procedures of non-biological complex drugs: a critical evaluation. *European Journal of Pharmaceutics and Biopharmaceutics*, **178**, 1-24 (2022) https://doi.org/10.1016/j.ejpb.2022.07.014

[24] Cunha S, Costa CP, Moreira JN, Lobo JM, Silva AC. Using the quality by design (QbD) approach to optimize formulations of lipid nanoparticles and nano emulsions: A review. *Nanomedicine: Nanotechnology, Biology and Medicine*, **28**, 102206 (2020) https://doi.org/10.1016/j.nano.2020.102206

[25] Beg S, Haneef J, Rahman M, Peraman R, Taleuzzaman M, Almalki WH. Introduction to analytical quality by design. InHandbook of Analytical Quality by Design 2021 Jan 1 (pp. 1-14). Academic Press. https://doi.org/10.1016/B978-0-12-820332-3.00009-1

[26] Alam MS, Srivastava N. Extraction, Phytochemical Characterization and Assessment of Antioxidant and Antimicrobial Properties of Callicarpa Longifolia. *Biochemical and Cellular Archives*, **25(1)**, 777-786 (2025) https://doi.org/10.51470/bca.2025.25.1.777

[27] Alam MS, Shrivastava N. Exploring key compounds in callicarpa longifolia: a study on isolation and identification. *Journal of Applied Pharmaceutical Research*, **13(1)**, 75-85 (2025) https://doi.org/10.69857/joapr.v13i1.751

[28] Sindhu RK, Gupta R, Wadhera G, Kumar P. Modern Herbal Nanogels: Formulation, Delivery Methods, and Applications. *Gels*, **8(2)**, 97 (2022) https://doi.org/10.3390/gels8020097

[29] Awlqadr FH, Majeed KR, Altemimi AB, Hassan AM, Qadir SA, Saeed MN, Faraj AM, Salih TH, Abd Al-Manhel AJ, Najm MA, Tsakali E. Nanotechnology-Based Herbal Medicine: Preparation, Synthesis, and Applications in Food and Medicine. *Journal of Agriculture and Food Research*, **19**, 101661 (2025) https://doi.org/10.1016/j.jafr.2025.101661

[30] Sharaf NS, Shetta A, Elhalawani JE, Mamdouh W. Applying Box-Behnken Design for Formulation and Optimization of PLGA-Coffee Nanoparticles and Detecting Enhanced Antioxidant and Anticancer Activities. *Polymers (Basel)*, **14(1)**, 144 (2021) https://doi.org/10.3390/polym14010144

[31] Alam P, Shakeel F, Taleuzzaman M, Foudah AI, Alqarni MH, Aljarba TM, Alshehri S, Ghoneim MM. Box-Behnken Design (BBD) application for optimization of chromatographic conditions in RP-HPLC method development for the estimation of thymoquinone in nigella sativa seed powder. *Processes*, **10(6)**, 1082 (2022) https://doi.org/10.3390/pr10061082

[32] Sisodiya S, Gautam S, Aneja D, Debnath M. Exploring the usage of Olive leaf and green synthesized Olive leaf metallic nanoparticles as soap supplement for the formulation and optimization of innovative germicidal herbal soap. *Industrial Crops and Products*, **219**, 119012 (2024) https://doi.org/10.1016/j.indcrop.2024.119012

[33] Luiz MT, Viegas JS, Abriata JP, Viegas F, de Carvalho Vicentini FT, Bentley MV, Chorilli M, Marchetti JM, Tapia-Blacido DR. Design of experiments (DoE) to develop and to optimize nanoparticles as drug delivery systems. *European Journal of Pharmaceutics and Biopharmaceutics*, **165**, 127-48 (2021) https://doi.org/10.1016/j.ejpb.2021.05.011

[34] Bala Chennaiah M, Kumar KD, Kumar BS, Tanneeru SR. Characterisation of zinc oxide nanoparticles–herbal synthesised coated with *Ocimum tenuiflorum*. *Advances in Materials and Processing Technologies*, **8(2)**, 466-77 (2021) https://doi.org/10.1080/2374068X.2021.1934642

[35] Altammar KA. A review on nanoparticles: characteristics, synthesis, applications, and challenges. *Frontiers in Microbiology*, **14,** 1155622 **(**2023) https://doi.org/10.3389/fmicb.2023.1155622

[36] Taleuzzaman M, Ahmed MM, Chattopadhyay M. Particle size role, Importance and Strategy of HPLC Analysis-An update. *Int Arch BioMed Clin Res.*, **2(2),** (2016) http://dx.doi.org/10.21276/iabcr.2016.2.2.2

[37] Kumari V, Tyagi P, Sangal A. In-Vitro kinetic release study of illicium verum (Chakraphool) polymeric nanoparticles. *Materials Today: Proceedings*, **60(1)**, 14-20 (2022) https://doi.org/10.1016/j.matpr.2021.11.014

[38] Santadkha T, Skolpap W, Thitapakorn V. Diffusion Modeling and in vitro release kinetics studies of curcumin-loaded superparamagnetic nanomicelles in cancer drug delivery system. *Journal of Pharmaceutical Sciences*, **111(6)**, 1690-99 (2022) https://doi.org/10.1016/j.xphs.2021.11.015

[39] Rahat I, Imam SS, Rizwanullah M, Alshehri S, Asif M, Kala C, Taleuzzaman M. Thymoquinone-entrapped chitosan-modified nanoparticles: formulation optimization to preclinical bioavailability assessments. *Drug Delivery*, **28(1)**, 973-84 (2021) https://doi.org/10.1080/10717544.2021.1927245

[40] Santadkha T, Skolpap W, Thitapakorn V. Diffusion Modeling and in vitro release kinetics studies of curcumin-loaded superparamagnetic nanomicelles in cancer drug delivery system. *Journal of Pharmaceutical Sciences*, **111(6),** 1690-99 (2022) https://doi.org/10.1016/j.xphs.2021.11.015

[41] Weng J, Tong HHY, Chow SF. In Vitro Release Study of the Polymeric Drug Nanoparticles: Development and Validation of a Novel Method. *Pharmaceutics*, **12(8),** 732 (2020) https://doi.org/10.3390/pharmaceutics12080732

[42] Varghese RM, Aravind Kumar S, Rajeshkumar S. Antibacterial activity of herbal formulation against common oral pathogens. *Bioinformation*, **19(5),** 663-669 (2023 https://doi.org/10.6026/97320630019663

[43] Varghese RM, Kumar A, Shanmugam R. Antimicrobial activity of zinc oxide nanoparticles synthesized using Ocimum tenuiflorum and Ocimum gratissimum herbal formulation against oral pathogens. *Cureus*, **16(2)**, e53562 (2024) https://doi.org/10.7759/cureus.53562

[44] Shanmugam R, Govindharaj S, Arunkumar P, Sanjana GS, Manigandan P, Sulochana G, Padmapriya A. Preparation of a herbal mouthwash with lemongrass and mint-mediated zinc oxide nanoparticles and evaluation of its antimicrobial and cytotoxic properties. *Cureus*, **16(2)**, e53671 (2024) https://doi.org/10.7759/cureus.53671

[45] Hossain TJ. Methods for screening and evaluation of antimicrobial activity: A review of protocols, advantages, and limitations. *European Journal of Microbiology and Immunology*, **14(2)**, 97-115 (2024) https://doi.org/10.1556/1886.2024.00035

[46] Mihailovic V, Sreckovic N, Nedic ZP, Dimitrijevic S, Matic M, Obradovic A, Selakovic D, Rosic G, Katanic Stankovic JS. Green synthesis of silver nanoparticles using Salvia verticillata and Filipendula ulmaria extracts: Optimization of synthesis, biological activities, and catalytic properties. *Molecules*, **28(2)**, 808 (2023) https://doi.org/10.3390/molecules28020808

[47] Choi S, Kang BS, Choi G, Kang M, Park H, Kim N, Chang PS, Kwak MK, Jeong HE, Jung HS. Multichamber PLGA Microparticles with Enhanced Monodispersity and Encapsulation Efficiency Fabricated by a Batch-Microfluidic Hybrid Approach. *Advanced NanoBiomed Research*, **3(10),** 2300044 (2023) https://doi.org/10.1002/anbr.202300044

[48] Li L, Li Z, Guo Y, Zhang K, Mi W, Liu J. Preparation of uniform-sized GeXIVA [1, 2]-loaded PLGA microspheres as long-effective release system with high encapsulation efficiency. *Drug Delivery*, **29(1),** 2283-95 (2022) https://doi.org/10.1080/10717544.2022.2089297

[49] Benavides Castillo L, Martinez Y. The concentration and type of emulsifier rules the oil/water and water/oil/water emulsion size distribution. *Chemical Engineering Communications*, **210(11),** 2064-71 (2023) https://doi.org/10.1080/00986445.2023.2169680

[50] Dong R, Wang F, Jing D, Liu Y, Bao Y. The Stirring Effect on the Crystal Morphology of p-Acetamidobenzoic Acid Solution Crystallization. *Crystals*, **15(3),** 284 (2025) https://doi.org/10.3390/cryst15030284

[51] Liaqat N, Jahan N, Khalil-Ur-Rahman, Anwar T, Qureshi H. Green synthesized silver nanoparticles: Optimization, characterization, antimicrobial activity, and cytotoxicity study by hemolysis assay. *Frontiers in Chemistry*, **10**, 952006 (2022**)** https://doi.org/10.3389/fchem.2022.952006

[52] Ryu S, Nam SH, Baek JS. Green Synthesis of Silver Nanoparticles (AgNPs) of Angelica Gigas Fabricated by Hot-Melt Extrusion Technology for Enhanced Antifungal Effects. *Materials (Basel)*, **15(20)**, 7231 (2022) https://doi.org/10.3390/ma15207231

[53] Akhtar K, Khan SA, Khan SB, Asiri AM. Scanning electron microscopy: Principle and applications in nanomaterials

characterization. *Springer International Publishing*, 113-145 (2018) https://doi.org/10.1007/978-3-319-92955-2_4

[54] Sarma SK, Dutta U, Bharali A, Kumar S, Baruah S, Sarma H, Laloo D, Sahu BP. Isolation of curcumin from Lakadong turmeric of Meghalaya and development of its PLGA-Cur-NS loaded nanogel for potential anti-inflammatory and cutaneous wound healing activity in Wistar rats. *Future Journal of Pharmaceutical Sciences*, **9(1),** 85 (2023) https://doi.org/10.1186/s43094-023-00534-9

[55] Manjunath AM, Priya S, Jyothi D. Mucoadhesive Chitosan-Coated PLGA Nanoparticles of Ashwagandha Extract for Colon-Targeted Delivery. *Ind. J. Pharm. Edu. Res.*, **57(4),** 971-82 (2023) http://dx.doi.org/10.5530/ijper.57.4.119

[56] Dalli M, El Guerraf A, Azizi SE, Benataya K, Azghar A, Mi-Kyung J, Maleb A, Bonglee K, Gseyra N. Loaded n-hydroxyapatite/SSG 3D scaffolds as a drug delivery system of nigella sativa fractions for the management of local antibacterial infections. *Nanomaterials*, **12(5),** 856 (2022) https://doi.org/10.3390/nano12050856

[57] Salim SA, Abed T, Abdelazim EB, Eissa NG, Elsabahy M, Kamoun EA. Exploring the Therapeutic Potential of Plant Extract-Loaded Polymeric Nanoparticles for Advanced Wound Healing: A Comprehensive Review. *Arabian Journal for Science and Engineering*, **13,** 1-9 (2025) https://doi.org/10.1007/s13369-025-10247-1

[58] Vladár AE, Hodoroaba VD. Characterization of nanoparticles by scanning electron microscopy. *Characterization of nanoparticles*, 7-27 (2020) https://doi.org/10.1016/B978-0-12-814182-3.00002-X

[59] Elumalai K, Srinivasan S, Shanmugam A. Review of the efficacy of nanoparticle-based drug delivery systems for cancer treatment. *Biomedical Technology*, **5**, 109-22 (2024) https://doi.org/10.1016/j.bmt.2023.09.001

[60] Khattab A, Nattouf A. Optimization of entrapment efficiency and release of clindamycin in microsponge based gel. *Scientific Reports*, **11(1)**, 23345 (2021) https://doi.org/10.1038/s41598-021-02826-7

[61] Fahmy OM, Eissa RA, Mohamed HH, Eissa NG, Elsabahy M. Machine learning algorithms for prediction of entrapment efficiency in nanomaterials. *Methods*, **218**, 133-40 (2023) https://doi.org/10.1016/j.ymeth.2023.08.008

[62] Baltz N, Scherließ R. Entrapment efficiency methodology for lipid nanoparticles-a literature review. *Open Nano*, 100251 (2025) https://doi.org/10.1016/j.onano.2025.100251

[63] Ewii UE, Attama AA, Olorunsola EO, Onugwu AL, Nwakpa FU, Anyiam C, Chijioke C, Ogbulie T. Nanoparticles for Drug Delivery: Insight Into In Vitro and In Vivo Drug Release from Nanomedicines. *Nano TransMed*, 100083 (2025) https://doi.org/10.1016/j.ntm.2025.100083

[64] Yang L, Wu W, Yang J, Xu M. Nanoparticle-mediated delivery of herbal-derived natural products to modulate immunosenescence-induced drug resistance in cancer therapy: a comprehensive review. *Frontiers in Oncology*, **15**, 1567896 (2025) https://doi.org/10.3389/fonc.2025.1567896

[65] Mehta J, Pathania K, Pawar SV. Recent overview of nanotechnolog based approaches for targeted delivery of nutraceuticals. *Sustainable Food Technology*, (2025) https://doi.org/10.1039/D5FB00122F

[66] Ezzariga N, Moukal A, Asdadi A, Lemkhente Z, Moustaoui F, Kaaya A, Aghrouch M. Evaluation of the Antimicrobial Activity of 20 Essential Oils and Their Combinations on Bacterial and Fungal Strains. *Cureus*, **17(2)**, e79499 (2025) https://doi.org/10.7759/cureus.79499

[67] Nagore P, Ghotekar S, Mane K, Ghoti A, Bilal M, Roy A. Structural properties and antimicrobial activities of Polyalthia longifolia leaf extract-mediated CuO nanoparticles. *BioNanoScience*, **11(2),** 579-89 (2021) https://doi.org/10.1007/s12668-021-00851-4

[68] Tourabi M, Metouekel A, Ghouizi AE, Jeddi M, Nouioura G, Laaroussi H, Hosen ME, Benbrahim KF, Bourhia M, Salamatullah AM, Nafidi HA. Efficacy of various extracting solvents on phytochemical composition, and biological properties of Mentha longifolia L. leaf extracts. *Scientific Reports*, **13(1),** 18028 (2023) https://doi.org/10.1038/s41598-023-45030-5